ELSEVIER

Journal of Molecular Catalysis B: Enzymatic 11 (2000) 97–112

JOURNAL OF MOLECULAR CATALYSIS B: ENZYMATIC

www.elsevier.com/locate/molcatb

The process of thermodialysis and the efficiency increase of bioreactors operating under non-isothermal conditions

N. Diano [a], M.M. El-Masry [a,1], M. Portaccio [b], M. Santucci [a], A. De Maio [a,b], V. Grano [a], D. Castagnolo [a,2], U. Bencivenga [a], F.S. Gaeta [a,2], D.G. Mita [a,b,*]

[a] *International Institute of Genetics and Biophysics of CNR, via Guglielmo Marconi, 12, 80125 Naples, Italy*
[b] *Department of Human Physiology and Integrated Biological Functions of the Second University of Naples, via S. M. di Costantinopoli, 16, 80138 Naples, Italy*

Received 8 May 2000; received in revised form 21 July 2000; accepted 21 July 2000

Abstract

When a catalytic membrane is employed in a non-isothermal bioreactor its activity increases as a direct function of the applied temperature gradient and decreases when both average temperature or substrate concentration increase. To know the physical cause responsible for this behaviour substrate fluxes have been studied under isothermal conditions (diffusion) and non-isothermal conditions (thermodialysis). Strong analogies between the behaviour of the catalytic membrane and the substrate fluxes produced by the process of thermodialysis have been observed. By introducing diffusive and thermodiffusive substrate fluxes in appropriate mass balance equations the substrate concentration profiles into the catalytic membrane have been deduced by computer simulation. In absence of catalysis and under non-isothermal conditions the profiles are higher than the ones corresponding under comparable isothermal conditions, while the contrary occurs in the presence of catalysis. The percentage increases of enzyme activity, calculated by the curves of the substrate concentration profiles, show the same temperature and concentration dependence than those actually observed with the catalytic membrane. The role of thermodialysis in affecting the enzyme activity in non-isothermal bioreactor has been discussed and demonstrated.

Keywords: Non-isothermal bioreactors; Thermodialysis; Catalytic membranes; Grafting; β-galactosidase

1. Introduction

During the last years it has been found that it is possible to increase the activity of enzymes immobilised on a membrane by interposing it between two equal substrate solutions maintained at different temperatures [1–13]. Activity increases were found also with immobilised quiescent cells when the activity of internal [4] or cell-wall [5] enzymes was studied. In all cases the presence of a hydrophobic membrane was requested. For this reason the observed effects were attributed to the process of thermodialysis [14–18], by which substrate crosses the catalytic membrane, interacting with the enzyme, under the action

* Corresponding author. Tel./fax: +39-81-2395887.
E-mail address: mita@iigbna.iigb.na.cnr.it (D.G. Mita).
[1] Present address: Department of Polymers and Pigments, National Research Center, Dokki, Cairo, Egypt.
[2] Mars Center, Via Comunale Tavernola, 80144 Naples, Italy.

1381-1177/00/$ - see front matter
PII: S1381-1177(00)00219-8

of thermal radiation forces [19–20] associated with the presence of a transmembrane temperature gradient.

Coupling between matter fluxes and temperature gradients is foreseen by the thermodynamics of irreversible processes [21–23] in bulk solution (thermal diffusion) and across membranes (thermoosmosis, pervaporation, thermodialysis).

Thermal diffusion in liquids [24,25], also known as Soret effect, is the process by which a temperature gradient generates a concentration gradient in a solution initially homogeneous.

Thermoosmosis [26–35] is the water transport under non-isothermal conditions across hydrophilic and charged membranes.

Pervaporation [36–39] is the transport from the warm to the cold side of a hydrophobic membrane of the component of a two liquid mixture having the higher vapour pressure. The driving force is the difference of the vapour pressure between the liquid phases wetting the two ends of the membrane channels, which remain empty of liquid owing to their hydrophobicity.

Thermodialysis [14–18] is the selective matter transport (some components drifting to cold, other to warm) across a hydrophobic porous membrane separating two liquid solutions crossed by a flux of thermal energy. The driving force is the thermal radiation force [19–20], proportional to the magnitude of the temperature gradient, which acts selectively on the components of a non-isothermal solution confined in the pores of a membrane. During the process of thermodialysis distinct fluxes of solutes and solvent are observed, as it will be seen in the following.

The aim of this work is to analyse the results obtained with a catalytic membrane in a bioreactor operating under isothermal and non-isothermal conditions, correlating the enzymatic response with the trasmembrane traffic of substrate produced by diffusion and/or by thermodialysis. The results relative to the enzyme activity are part of those reported in reference n° 40. Experiments relative to lactose transport by diffusion and/or thermodialysis have been performed to obtain information about some physical parameters necessary to derive the substrate concentration profile into the catalytic membrane.

2. Apparatus, materials and methods

2.1. The reactor

The reactor employed, shown in Fig. 1, consists of two metallic flanges in each of which a shallow cylindrical cavity, 70 mm in diameter and 2.5 mm deep, was bored. A membrane is interposed between the two half-cells, containing the solution. By means of external thermostats, both the half-cells and their liquid content are thermostatted at predetermined temperatures, measured by thermocouples positioned at 1.5 mm from the membrane surfaces. In this way it is possible to know the average temperature of the apparatus, $T_{av} = [T_w + T_c]/2$, and the applied temperature difference $\Delta T = T_w - T_c$. Subscripts 'w' and 'c' are for warm and cold, respectively. The reactor

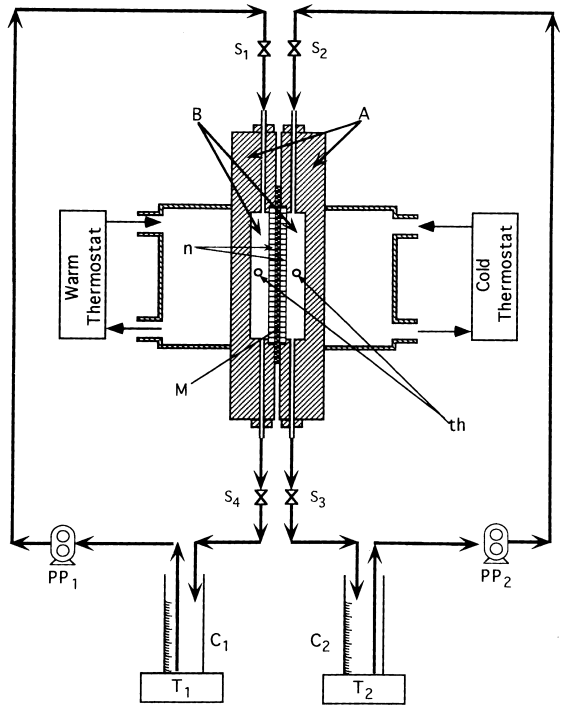

Fig. 1. Schematic (not to scale) representation of the bioreactor. A, half-cells; B, internal working volumes; M, membrane; n, supporting nets; th, thermocouples; S_i, stopcocks allowing the apparatus to work under different conditions; T_i, thermostatic magnetic stirrers, C_i, external working volumes; PP_i, peristaltic pumps.

can be used under various conditions: (a) closed working volumes; (b) one half-cell with closed working volume (usually the cold overpressurized one) and the other with recirculation of the working solution; (c) both half-cells with the working solutions recirculated in independent hydraulic circuits through the C_1 and C_2 cylinders.

Under the (a) condition, employing aqueous solutions, volume and concentration changes in the cold and warm half-cells are observed. In particular, thermodialysis induces thermoosmotic water transport in the cold half-cell and differential solute transport towards the warm or the cold solution in dependence on its nature. The thermoosmotic water flow stops when in the cold half-cell a thermoosmotic pressure is developed, generating a hydraulic water counterflow equal to the one produced by the temperature gradient.

Under the (b) condition, having suitably overpressured the cold half-cell, water transport is not observed, but solute fluxes occur, generally towards the warm half-cell.

When the apparatus works under (c), with the two hydraulic circuits starting and ending in the respective cylinders C_1 and C_2, volume and concentration changes are allowed.

The (b) and (c) conditions have been employed in this research.

2.2. Materials

The membrane used was obtained by chemical grafting butylmethacrylate (BMA) on a nylon hydrolon membrane manufactured by Pall (Pall Italia, Milano, Italy). Hexamethylenediamine and glutaraldehyde were also used according to the procedures described elsewhere [40]. Enzyme immobilisation was not done.

All chemicals, including lactose, were purchased from Sigma Chemical Company (St. Luis, MO) and used without further purification. Lactose concentration was determined by sampling at regular time intervals the solution in the two cylinders and converting the lactose content in glucose and galactose by β-galattosidase (E C 3.2.1.23). At the end of this procedure the glucose concentration, proportional to lactose concentration, is measured with the GOD-Perid test (Boheringer GmbH, Mannheim, Germany), according to the methodology described in reference n° 40.

2.3. Methods

2.3.1. Diffusion experiments

Diffusion experiments have been carried out with one half-cell filled with lactose solution and the other one with pure water. The contents of each half-cell were recirculated in independent hydraulic circuits starting and ending in two separate cylinders. Glucose/lactose concentrations in each half-cell were determined by sampling at regular time intervals the solution in the corresponding cylinder. Average diffusive fluxes in the time interval Δt were calculated by means of the expression:

$$J_{\text{diff}} = \frac{\Delta n}{A\Delta t} = \frac{V}{A\Delta t}\left|C(t) - C(t+\Delta t)\right| \qquad (1)$$

J_{diff} being expressed in moles $\text{cm}^{-2}\,\text{s}^{-1}$; V is the volume of each working solution, in cm^3; A the working membrane area, in cm^2; Δt is in seconds; and C is the concentration, in moles cm^{-3}.

Having calculated the average fluxes at different times, the initial lactose diffusive flux J^0_{diff} is obtained by extrapolating these fluxes to zero time.

The value of the diffusion coefficient D^* ($\text{cm}^2\,\text{s}^{-1}$) is then obtained by means of the equation

$$J^0_{\text{diff}} = D^* \frac{\Delta C}{\Delta x} \qquad (2)$$

where $\Delta C/\Delta x$ (moles cm^{-4}) is the concentration gradient cross the membrane having thickness Δx.

2.3.2. Thermodialysis experiments

Thermodialysis was performed in presence and in absence of water fluxes produced by temperature gradients. In the first case, condition (c), two independent hydraulic circuits allowed solution recirculation in the two half-cells as in diffusion experiments; in the second case the reactor was operating under the condition (b). In the first case changes of volumes and concentrations of working solutions in the two half-cells and in the respective cylinders were

observed. The volume flux ($cm^3\,cm^{-2}\,s^{-1}$) is calculated by means of the expression

$$J_v = \frac{\Delta V}{A\Delta t} \tag{3}$$

where ΔV (cm^3) is the volume transported in the time interval Δt.

The apparent solute fluxes, $J_{s,app}$ (moles $cm^{-2}\,s^{-1}$), are calculated by knowing during time the moles in each half-cell, these moles being $n(t) = C(t)\,V(t)$. The expression for $J_{s,app}$ therefore is

$$J_{s,app} = \frac{1}{A}\left|\frac{\Delta n}{\Delta t}\right|_{w,c} = \frac{1}{A}\left|\frac{[n]_{t+\Delta t} - [n]_t}{\Delta t}\right|_{w,c} \tag{4}$$

where the symbol $|_{w,c}$ means that the fluxes can be calculated indifferently in the warm or cold half-cell. By calculating in this way the apparent average fluxes at different times and by extrapolating to zero time the curve of the average fluxes versus time, it is possible to obtain the initial apparent solute flux. This flux is called apparent since it is given by

$$J^0_{s,app} = J_{s,drag} + J_{s,td} \tag{5}$$

This expression indicates that the apparent flux is the algebraic sum of two distinct fluxes. $J_{s,drag}$, directed from the warm to the cold half-cell, is the solute flux associated to the volume transport and $J_{s,td}$, which is produced by a modified thermal diffusion into the membrane pores. The direction of the latter flux depends on the nature of solute and solvent.

$J_{s,drag}$ is calculated by means of the equation

$$J_{s,drag} = J_v C_w = v_{H_2O} C_w \tag{6}$$

where J_v is the volume flux defined by Eq. (3) and C_w is the concentration in the warm half-cell from which the volume flux is coming. v_{H_2O}, expressed in $cm\,s^{-1}$, is the rate of water transport from the warm to the cold half-cell and its value is equal to J_v

It is possible to calculate $J_{s,td}$ by means of Eq. (5) knowing the relative directions of the other two fluxes.

An independent way to measure $J_{s,td}$ comes from thermodialysis experiments in absence of volume flux, i.e. with the cold half-cell closed and overpressured. By measuring the concentration changes in the warm half-cell in the course of time, $J_{s,td}$ is calculated by means of the equation

$$J_{s,td} = \frac{1}{A}\left|\frac{\Delta n}{\Delta t}\right|_w = \frac{1}{A}V_w\left|C(t+\Delta t) - C(t)\right|_w \tag{7}$$

where V_w is the volume of the warm solution, constant during time. By calculating $J_{s,td}$ at different times and by extrapolating to zero time the curve of the average fluxes versus time, it is possible to obtain the initial value of $J^0_{s,td}$. The value of the thermal diffusion coefficient D^*_{td} ($cm^2\,s^{-1}\,K^{-1}$) is obtained by means of the expression

$$J^0_{s,td} = D^*_{td} C_0 \frac{\Delta T}{\Delta x} \tag{8}$$

where C_0 is the initial solute concentration and $\Delta T/\Delta x$ the transmembrane temperature gradient ($K\,cm^{-1}$).

2.3.3. Temperature profile across the membrane

To estimate the actual effects of temperature gradients in processes occurring across membranes the temperatures on the membrane surfaces must be known. Since their measure is not possible, we have calculated these temperatures by means of Fourier

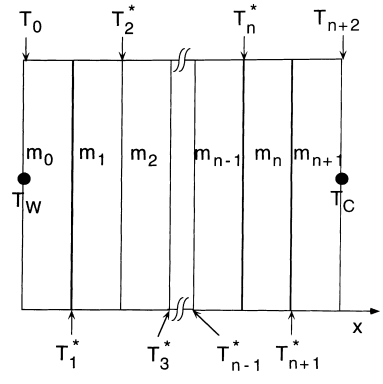

Fig. 2. A multimembrane system (n components) interposed between two liquid solutions, m_0 and $m_n + 1$, maintained at two different temperatures $T_w = T_0 > T_c = T_n + 2$.

Table 1
Volume and substrate fluxes obtained at different initial substrate concentrations under non-isothermal conditions defined by $T_{av} = 25°C$ and $\Delta T = 30°C$[a]

C (mM)	$J_{s,td} \times 10^{11}$ (moles cm^{-2} s^{-1})	$J_v \times 10^5$ (cm s^{-1})	$J_{s,drag} \times 10^9$ (moles cm^{-2} s^{-1})	$J_{s,obs} \times 10^9$ (moles cm^{-2} s^{-1})	$J_{s,td}^{calc} \times 10^{11}$ (moles cm^{-2} s^{-1})
15	0.56	3.58	0.54	0.54	0.40
30	1.13	3.56	1.07	1.06	1.01
50	1.87	3.54	1.77	1.74	2.99
75	2.82	3.51	2.63	2.60	3.21
100	3.74	3.48	3.48	3.44	3.56
150	5.61	3.43	5.14	5.09	4.89
200	7.48	3.36	6.72	6.65	7.19
250	7.48	3.30	8.25	8.17	7.99
300	11.21	3.24	9.72	9.62	10.20

[a] Fluxes in the columns have the meaning described in the text.

law for heat conduction. This is possible since in our case the liquid motion in each half-cell, constrained at a rate of 2.5 cm^3 min^{-1} between two fins with rounded tips, is laminar (11) and fluid flow occurs within isothermal planes, normal to the temperature gradient. Thus, heat propagation in the reactor occurs by conduction between isothermal liquid planes perpendicular to the direction of heat flow. In this way, starting from the consideration that

$$J_{q,i} = -K_i \left(\frac{\Delta T}{\Delta x} \right)_i = J_q = \text{constant} \tag{9}$$

through all the media crossed by heat flow, i.e. liquids (solutions) and solids (membranes), confined between the two half-cells, the temperatures on each membrane surface constituting the membrane system can be calculated. In Eq. (9) $J_{q,i}$ represents the heat flux across the i-th medium, Δx_i thick, subject to a temperature difference ΔT_i and having thermal conductivity K_i. If the membrane system is composed of n membranes, as in Fig. 2, $(n + 2)$ equations similar to (9) can be written considering also the two liquid solutions filling each half-cell. These equations are

$$T_{i-1} - T_i = J_q \frac{x_{i-1} - x_i}{K_{i-1}} \tag{10}$$

with $i = 1, \ldots, n + 2$ and $T_0 = T_w$ and $T_{n+2} = T_c$, i.e. the temperatures read by the thermocouples in the warm and cold half-cell, respectively. Owing to the continuity of heat flow, by summing all the equations derived from Eq. (10) it is possible to calculate J_q as

$$J_q = \frac{T_0 - T_{n+2}}{\sum_{i=1}^{n+2} (x_i - x_{i-1})/K_{i-1}} \tag{11}$$

Once known J_q, the temperature T_i^* on the surface of i-th membrane is calculated by solving each single equation indicated in Eq. (10). In this way, knowing T_w and T_c, the actual temperatures on each surface of the n-membranes are obtained by means of Eqs. (10) and (11). Calling $T_{w,i}^*$ and $T_{c,i}^*$ the temperatures on warm and cold surfaces of the i-th membrane, it is evident that $T_{w,i}^* < T_w$, and $T_{c,i}^* > T_c$, thus $\Delta T_i^* = T_{w,i}^* - T_{c,i}^* < \Delta T = T_w - T_c$.

Using a single membrane, as in the present case, the temperatures reported in Table 1 of reference n° 40 have been calculated.

3. Results and discussion

All experimental points reported in the figures are the average of six independent experiments carried out under the same conditions. The experimental errors never exceeded 8%.

Diffusion and thermodialysis experiments have been programmed to explain the activity increase of a catalytic membrane crossed by a flux of thermal

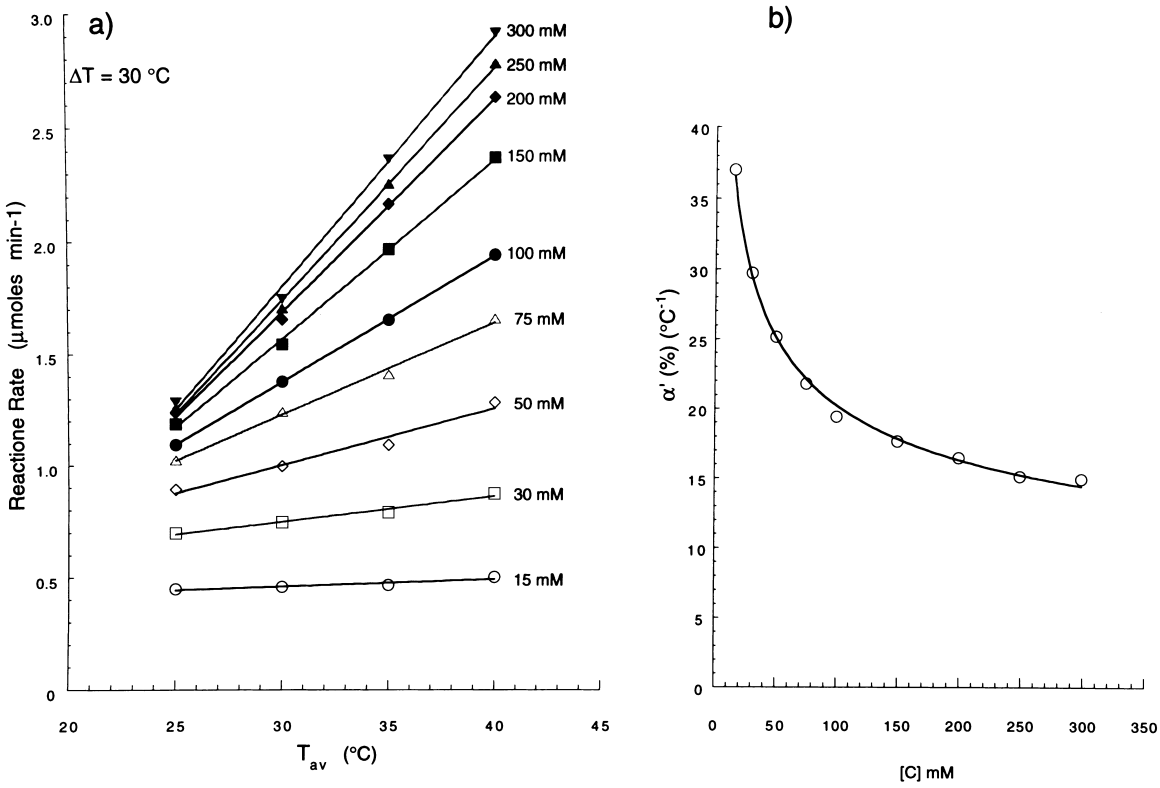

Fig. 3. (a) Enzyme reaction rate as a function of T_{av} under non-isothermal conditions, at $\Delta T = 30°C$. Curve parameter is substrate concentration. Symbols: 15 mM (○); 30 mM (□); 50 mM (◇); 75 mM (△); 100 mM (●); 150 mM (■); 200 mM (♦); 250 mM (▲); 300 mM (▼); (b) percentage increase of the enzyme reaction rate as a function of substrate concentration at $T_{av} = 25°C$ and $\Delta T = 30°C$.

energy. In particular they have been addressed to explain the results reported in Fig. 3. These results constitute a portion of a paper [40] dealing with the concentration dependence of the percentage activity increase, α', of a catalytic membrane employed in a non-isothermal bioreactor. The percentage activity increase α' has been defined as:

$$\alpha' = \frac{\mathrm{RR}|_{\Delta T^* \neq 0}^{T_{av}^*} - \mathrm{RR}|_{\Delta T^* = 0}^{T_{av}^*}}{\mathrm{RR}|_{\Delta T^* = 0}^{T_{av}^*}} \frac{1}{\Delta T^*} \qquad (12)$$

where $\mathrm{RR}|_{\Delta T^* \neq 0}^{T_{av}^*}$ and $\mathrm{RR}|_{\Delta T^* = 0}^{T_{av}^*}$ represent the reaction rates (RR) of the catalytic membrane at $T = T_{av}^*$ under isothermal and non-isothermal conditions, respectively.

The role of the process of thermodialysis in increasing the activity of a catalytic membrane operating under non-isothermal conditions will be demonstrated if the study of substrate transport across the membrane under isothermal and non-isothermal conditions will give results correlable with expression (12).

3.1. Isothermal diffusion experiments

In Fig. 4 the diffusive lactose fluxes at $T = 25°C$ have been reported as a function of the transmembrane concentration gradient. For clarity in the upper scale the lactose transmembrane concentration difference has been added. The angular coefficient of the straight line best fitting the experimental points gives the diffusion coefficient D^* across the membrane, which is equal to $1.04 \times 10^{-7}\,\mathrm{cm^2\,s^{-1}}$.

Analogous experiments at different temperatures gave the following values for D^*: $1.24 \times 10^{-7}\,\mathrm{cm^2\,s^{-1}}$ at $T = 30°C$; $1.45 \times 10^{-7}\,\mathrm{cm^2\,s^{-1}}$ at $T = 35°C$ and $1.63 \times 10^{-7}\,\mathrm{cm^2\,s^{-1}}$ at $T = 40°C$.

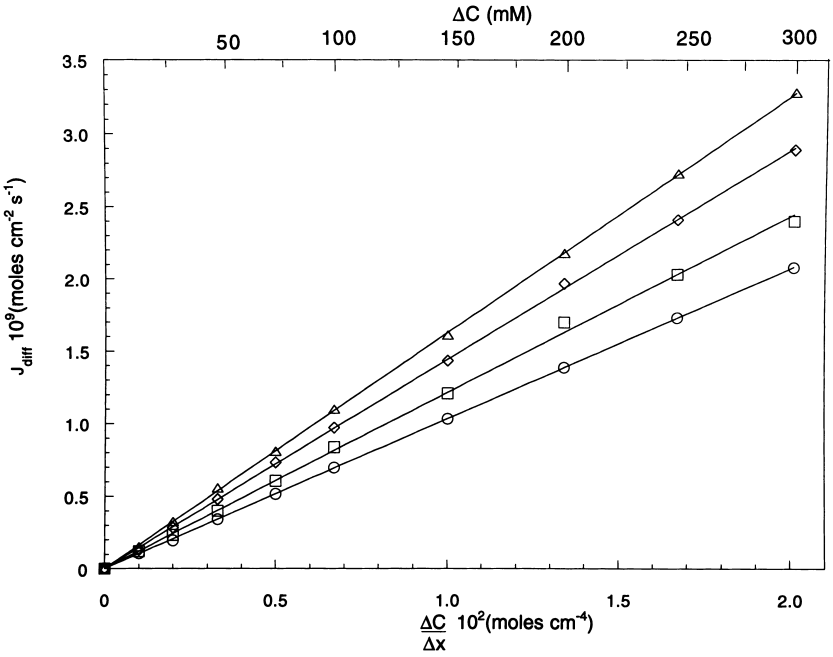

Fig. 4. Diffusive substrate fluxes as a function of concentration gradient. Curve parameter is the temperature. Symbols: $T = 25$°C (○); $T = 30$°C (□); $T = 35$°C (◇); $T = 40$°C (△).

3.2. Thermodialysis experiments

Results relative to experiments carried out under temperature gradients are grouped into two sections: (a) experiments with the cold half-cell overpressured and solution recirculation in the warm half-cell; (b) experiments with solution recirculation in both half-cells by means of hydraulic circuits starting and ending in two separate cylinders.

3.2.1. Experiments with the cold half-cell overpressured and solution recirculation in the warm half-cell

When the reactor works under these conditions only a modified 'thermal diffusion' in the membrane pores occurs since volume flow, which is always directed to the cold half-cell, is forbidden. Following the concentration changes in the warm half-cell during time, it is possible to calculate the 'thermodiffusive' lactose fluxes, $J_{s,td}$, by means of the procedure described in 2.3.2. In Fig. 5a $J_{s,td}$ fluxes are reported as a function of the initial lactose concentration. Experiments have been performed at $T_{av} = 25$°C and different ΔT's, which are curve parameters. From this figure it is possible to see that thermodiffusive fluxes increase with the initial lactose concentration and with the applied ΔT. The linearity between 'thermodiffusive' fluxes and ΔT is better appreciated in Fig. 5b where lactose fluxes are reported as a function of applied temperature gradients only for some initial concentrations which are the curve parameter. The angular coefficients (moles cm^{-1}-s^{-1} K^{-1}) of the straight lines best fitting the experimental points of Fig. 5b divided by the corresponding lactose concentration (moles cm^{-3}) give the value of the thermal diffusion coefficients D^*_{td} (cm^2 s^{-1} K^{-1}) in the membrane pores which, in our case, turns out to be 1.84×10^{-10} cm^2 s^{-1} K^{-1}. A correction must be introduced in the D^*_{td} value considering the actual value of the temperature difference across the membrane reported in Table 1 of reference [40]. This correction is easily made by multiplying the value of D^*_{td} for the ratio $\Delta T/\Delta T^*$. In the present case, $\Delta T/\Delta T^*$ is equal to 12.5. Accounting for this correction the lactose thermal diffusion coefficient across the membrane becomes $D^*_{td} = 2.30 \times 10^{-9}$ cm^2 s^{-1} K^{-1} at $T_{av} = 25$°C.

Analogous experiments gave the following values for D^*_{td} at other average temperatures: $2.83 \times$

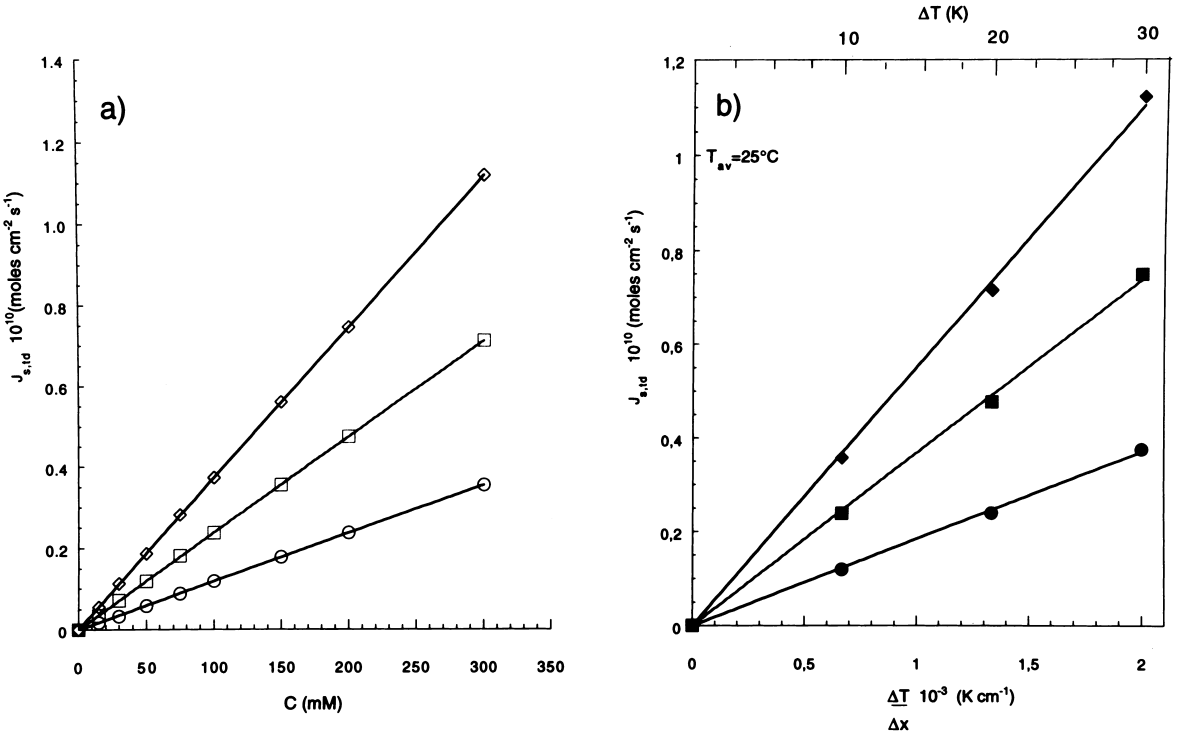

Fig. 5. Thermodiffusive substrate fluxes as a function of the substrate concentration (a) and temperature gradient (b). Symbols: $\Delta T = 10$°C (○); $\Delta T = 20$°C (□); $\Delta T = 30$°C (◇); 100 mM (●); 200 mM (■); 300 mM (◆).

10^{-9} cm^2 s^{-1} K^{-1} at $T_{av} = 30$°C; 3.36×10^{-9} cm^2 s^{-1} K^{-1} at $T_{av} = 35$°C; 3.79×10^{-9} cm^2 s^{-1} K^{-1} at $T_{av} = 40$°C.

3.2.2. Experiment with the solutions recirculated in both half-cells by means of independent hydraulic circuits

As reported in Section 2.3.2 during these experiments volume and concentration changes are observed. Measuring these parameters in the course of time it is possible to calculate volume and lactose fluxes according to Eqs. (3) and (4), respectively. In Fig. 6 these fluxes are reported as a function of the initial lactose concentration. The curve parameter is the macroscopic temperature difference. Fig. 6a refers to volume fluxes directed towards the cold half-cells. Fig. 6b refers to the observed lactose fluxes, directed towards the warm half-cells.

Remembering that $J_{s,obs} = J_{s,drag} + J_{s,td}$ from the fluxes in Fig. 6 it is possible to calculate the lactose thermal diffusive fluxes $J_{s,td}^{calc}$, remembering that all fluxes are vectorial. These fluxes, reported in the sixth column of Table 1, agree with the ones measured $J_{s,td}$ (second column) according to the methodology reported in 3.2.1.

3.3. Analogies between substrate fluxes in thermodialysis and activity increases of the catalytic membrane under non-isothermal conditions

Experiments similar to those reported in Fig. 6 have also been carried out at different average temperatures, such as 30, 35 and 40°C. In Fig. 7 lactose fluxes are reported as a function of T_{av}, under constant $\Delta T = 30$°C. Fig. 7a refers to J_{drag} and Fig. 7b to $J_{s,td}$. In both figures the curve parameter is the initial lactose concentration. A remarkable analogy emerges when the results in Fig. 7 are compared to those reported in Fig. 3a. Both figures show a linear dependence from the average temperature with angular coefficients increasing with the increase of the initial concentration. In Table 2 the angular coeffi-

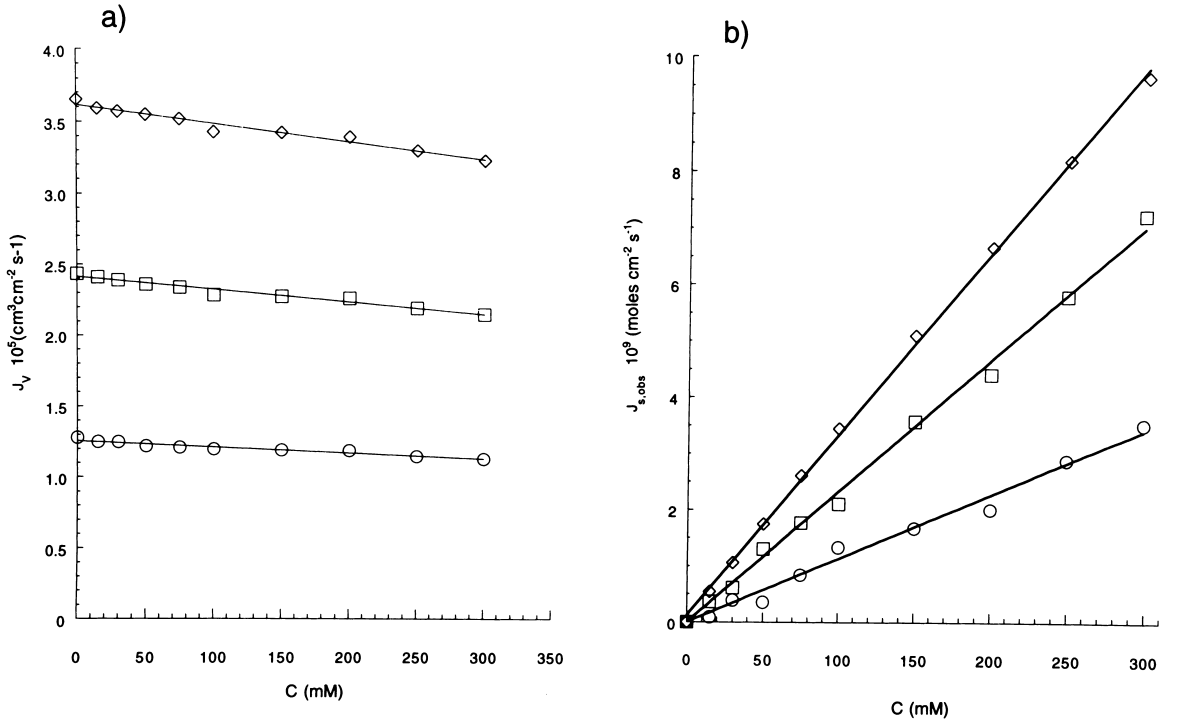

Fig. 6. Volume fluxes (a) and observed lactose fluxes (b) as a function of substrate concentrations. Curve parameter is the applied ΔT. Symbols: $\Delta T = 10°C$ (○); $\Delta T = 20°C$ (□); $\Delta T = 30°C$ (◇).

cients of the straight lines best fitting the experimental points of Figs. 3a and 7 are reported. These stringent analogies indicate that a common physical phenomenon is at the basis of the observed effects, this phenomenon being the lactose traffic produced by a flux of thermal energy across a hydrophobic membrane, catalytic or not.

These analogies become more significative if the behaviour of Fig. 3b can be explained in terms of lactose/substrate traffic under isothermal and non-isothermal conditions across the catalytic membrane. To do this we shall employ simple mass balance equations into the membrane thickness.

3.4. Substrate concentration profile into the membrane

The results reported in figures from 4 to 7 allow us to calculate the substrate concentration profiles within the membrane under isothermal and non-isothermal conditions in the presence or in the absence of catalysis. To do this the mass balance for lactose into an elementary volume of thickness Δx of our membrane must be carried out, according to the equation:

$$\{\text{Rate of input}\} - \{\text{Rate of output}\} - \{\text{Rate of consumption by enzyme reaction}\} = \{\text{Rate of accumulation}\} \quad (13)$$

Each member of the equation is measured in moles s^{-1}.

To understand the nature of the fluxes crossing the membranes reference must be made to Fig. 8, representing the membrane separating two lactose solutions at concentration C_0, kept at temperatures T_1 and T_2, respectively. The elementary volume between x and $x + \Delta x$ is also represented. Fig. 8a illustrates the isothermal case, Fig. 8b the non-isothermal one.

3.4.1. Isothermal case

With reference to this case the temperatures T_1 and T_2 are equal.

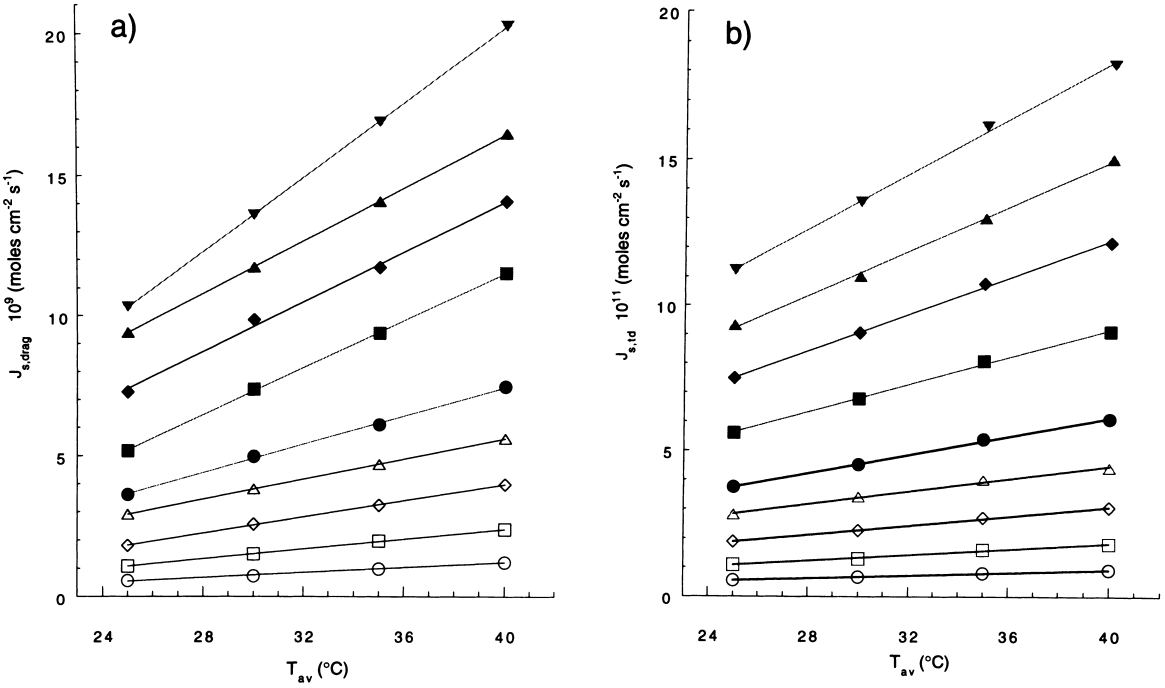

Fig. 7. Lactose drag (a) and thermodiffusive fluxes (b) as a function of the average temperature. Curve parameter is the substrate concentration. Symbols: 15 mM (○); 30 mM (□); 50 mM (◇); 75 mM (△); 100 mM (●); 150 mM (■); 200 mM (♦); 250 mM (▲); 300 mM (▼).

When the general Eq. (13) is put in analytic form one has:

$$J_{\text{diff}}|_x A - J_{\text{diff}}|_{x+\Delta x} A - \frac{V_m C(x,t)}{K_m + C(x,t)} A\Delta x = \frac{\Delta C(x,t)}{\Delta t} A\Delta x \qquad (14)$$

where A is the membrane area in cm^2; J_{diff} are the substrate diffusive fluxes, expressed in moles cm^{-2} s^{-1}, across the surfaces of our elementary volume at positions x and $x+\Delta x$; $V_m C(x,t)/(K_m + C(x,t))$, expressed in moles cm^{-3} s^{-1}, is the substrate consumption by the enzyme reaction characterised by the kinetic parameters V_m and K_m measured in moles cm^{-3} s^{-1} and in moles cm^{-3}, respectively; C is the substrate concentration in moles cm^{-3} and $\Delta C(x,t)/\Delta t$ indicates the substrate accumulation, in moles cm^{-3} s^{-1}. V_m, is related to unit membrane volume.

Upon division by $A\,\Delta x$ and substitution of J_{diff} with $-D^*\Delta C/\Delta x$ (Fick law), for $\Delta x \to 0$ and $\Delta t \to 0$ the following second order differential equation for the variable $C(x,t)$ is obtained:

$$D^* \frac{\partial^2 C(x,t)}{\partial x^2} - \frac{V_m C(x,t)}{K_m + C(x,t)} = \frac{\partial C(x,t)}{\partial t} \qquad (15)$$

The boundary conditions are: $C(x,0) = 0$; $C(0,t) = C_0$; $C(d,t) = C_0$. According to the first condition, when $t = 0$, there is no substrate into the membrane; the second and third conditions establish that the concentration on the two surfaces of the membrane has, at any time, the constant value C_0. Besides these conditions we also assume that: (a) the reaction heat is negligible; (b) D^* is constant and independent from substrate concentration; (c) the substrate concentration in external working solution is generally low and product reaction does not affect diffusion; (d) enzymes are distributed uniformly within the

Table 2
In the second, third and fourth column the angular coefficients of the lines reported in Figs. 3a, 7a and b, are listed as a function of the initial lactose concentration (first column)[a]

C (mM)	Angular coefficient $\Delta RR/\Delta T_{av}$ (μmoles min^{-1}°C^{-1})	Angular coefficient $\times 10^{10}$ $\Delta J_{s,drag}/\Delta T_{av}$ (moles cm^{-2} s^{-1}°C^{-1})	Angular coefficient $\times 10^{12}$ $\Delta J_{s,td}/\Delta T_{av}$ (moles cm^{-2} s^{-1}°C^{-1})
15	0.003	0.42	0.24
30	0.012	0.89	0.49
50	0.026	1.44	0.78
75	0.042	1.79	1.08
100	0.059	2.50	1.57
150	0.080	4.23	2.36
200	0.095	4.48	3.14
250	0.103	4.70	3.82
300	0.111	6.58	4.71

[a] The experimental conditions are: $T_{av} = 25$°C and $\Delta T = 30$°C.

membrane; (e) substrate concentration inside the membrane depends only on position along x.

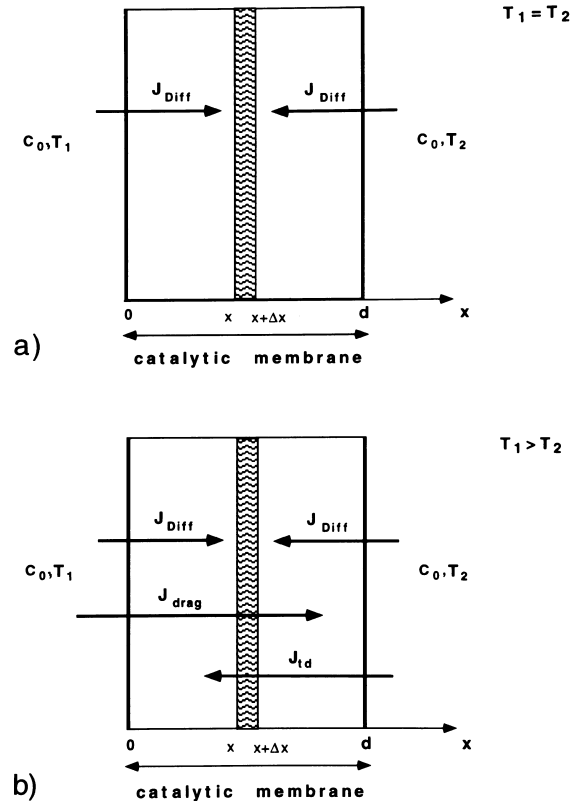

Fig. 8. Schematic representation of substrate fluxes into the membrane and, hence, into the elementary volume of thickness Δx, under isothermal (a) and non-isothermal (b) conditions.

By solving Eq. (15) the substrate concentration profile into the membrane under isothermal conditions is obtained. In Fig. 9 the substrate concentration profile (full lines) is represented for the isothermal case $T = 25$°C as obtained by a simulation program for second order differential non linear equations, under the condition that $\partial C(x,t)/\partial t \leq 5 \times 10^{-6}$ moles cm^{-3} s^{-1}. The values of the kinetic parameters have been taken from reference n° 40.

3.4.2. Non-isothermal case

Let us consider now the case where the two solutions bathing the catalytic membrane are kept at different temperatures T_1 and T_2, with $T_1 > T_2$.

Under isothermal conditions the substrate traffic across the catalytic membrane is due only to diffusion. Under non-isothermal conditions substrate fluxes produced by thermodialysis add to the diffusive ones. It must also be remembered that the fluxes produced by the process of thermodialysis are: a flux from cold to warm ($J_{s,td}$) and a flux in opposite direction ($J_{s,drag}$) dragged by the solvent flow. Accordingly, the mass balance equation in our elementary volume Δx thick is given by:

$$J_{diff}|_x A - J_{diff}|_{x+\Delta_x} A + J_{s,drag}|_x A - J_{s,drag}|_{x+\Delta x} A + J_{s,td}|_{x+\Delta_x} A - J_{s,td}|_x A - \frac{V_m^* C(x,t)}{K_m^* + C(x,t)} A \Delta x = \frac{\Delta C(x,t)}{\Delta t} A \Delta x \quad (16)$$

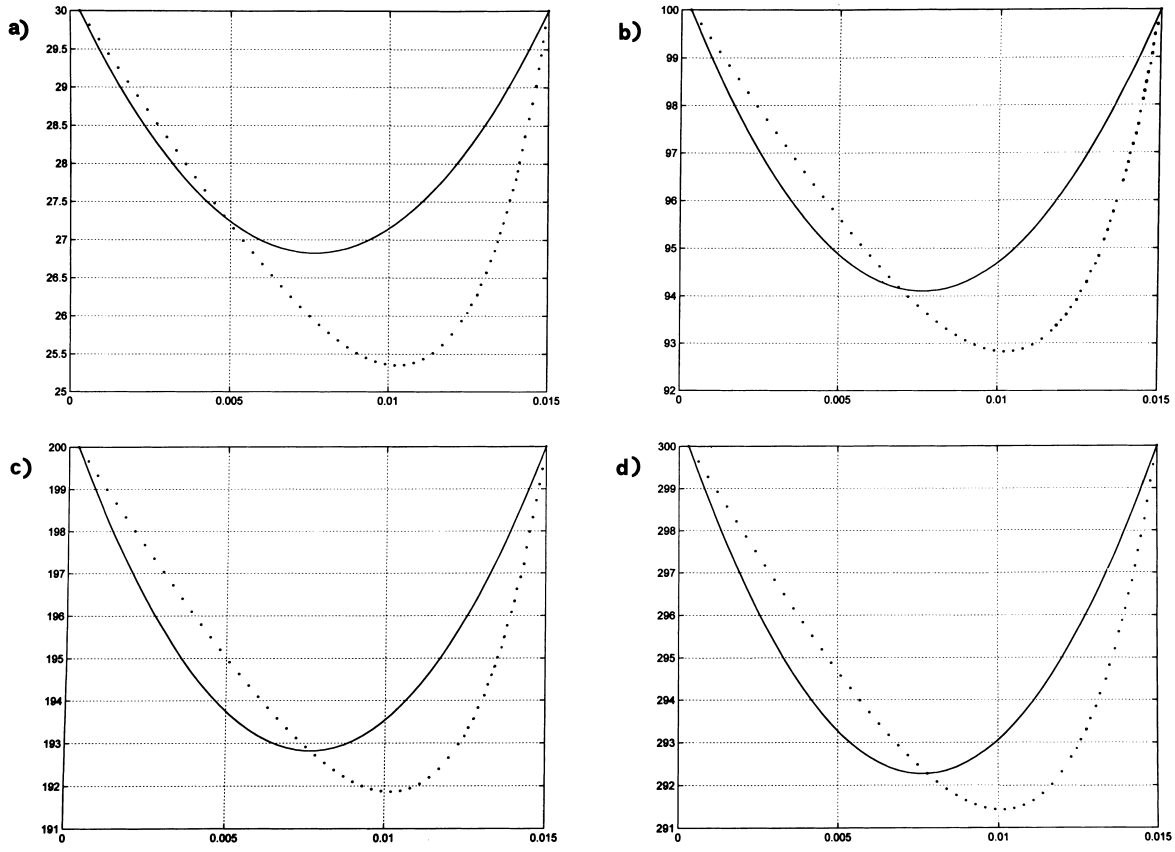

Fig. 9. Lactose concentration profiles into the membrane in presence of catalysis under isothermal (full lines) and non-isothermal (dotted lines) conditions. Initial lactose concentrations: (a) 30 mM; (b) 100 mM; (c) 200 mM; (d) 300 mM. On the y axis are reported the concentrations (mM) and on the x axis the membrane thickness.

where each term, expressed in moles s^{-1}, has the usual meaning.

Upon division by $A\,\Delta x$ and substitution of J_{diff}, J_{drag} and $J_{s,td}$ with the Fick law and the expressions (6) and (7), respectively, for $\Delta x \to 0$ and $\Delta t \to 0$ the second following order differential equation for the variable $C(x,t)$ is obtained:

$$D^* \frac{\partial^2 C(x,t)}{\partial x^2} - \left(V_{H_2O} - D^*_{td} \frac{\Delta T^*}{\Delta x} \right) \frac{\partial C(x,t)}{\partial x} - \frac{V^*_m C(x,t)}{K^*_m + C(x,t)} = \frac{\partial C(x,t)}{\partial t} \quad (17)$$

whose boundary conditions are equal to those of Eq. (15). V^*_m and K^*_m are the values of the kinetic parameters of the enzyme reaction obtained under non-isothermal conditions. Also in this case conditions from (a) to (e) still stand; in addition V_{H_2O} and $\Delta T^*/\Delta x$ are also considered constant with position.

Putting $(v_{H_2O} - D^*_{td}(\Delta T^*/\Delta x)) = K$, Eq. (17) becomes

$$D^* \frac{\partial^2 C(x,t)}{\partial x^2} - K \frac{\partial C(x,t)}{\partial x} - \frac{V^*_m C(x,t)}{K^*_m + C(x,t)} = \frac{\partial C(x,t)}{\partial t} \quad (18)$$

When $K = 0$, i.e. in absence of thermodialysis, Eq. (18) reduces to Eq. (15), i.e to the equation for the isothermal case.

By solving Eq. (17) through the simulation program, it is possible to obtain the concentration profile within the membrane, under the condition that $\partial C(x,t)/\partial t \leq 5 \times 10^{-6}$ moles $cm^{-3}\,s^{-1}$. In Fig. 9

the substrate concentration profiles (dotted lines) under non-isothermal conditions defined by $T_{av} = 25°C$ and $\Delta T = 30°C$ are reported for four different initial lactose concentrations. The values of the kinetic parameters have been taken from reference [40]. Inspection of each plot in Fig. 9 shows that the lactose concentration profile under non-isothermal conditions is altogether lower than that obtained under isothermal ones, indicating in this way an increase of the enzyme reaction rate, with a consequent increase of substrate consumption rate, when a temperature gradient is present.

When $V_m C(x,t)/(K_m + C(x,t))$ and $V_m^* C(x,t)/(K_m^* + C(x,t))$ are both put equal to zero, i.e. in absence of catalysis, the concentration profiles of Fig. 10 are obtained. Also in this case computer simulation was carried out under the condition $\partial C(x,t)/\partial t \leq 5 \times 10^{-6}$ moles cm^{-3} s^{-1}. It is easy to see that the relative positions of full versus dotted lines are opposite with respect to Fig. 9. From Fig. 9 one may calculate the areas enclosed between each curve and the horizontal axis giving the initial substrate concentration. These areas clearly represent substrate consumption due to enzymatic activity and, consequently, are equivalent to the glucose production in the process. The ratio

$$\beta = \frac{[\text{area}]_{\Delta T^* \neq 0}^{T_{av}^*} - [\text{area}]_{\Delta T^* = 0}^{T_{av}^*}}{[\text{area}]_{\Delta T^* = 0}^{T_{av}^*} \Delta T^*} \tag{19}$$

calculated from the graphs of Fig. 9 therefore represents the activity percentage increase due to the

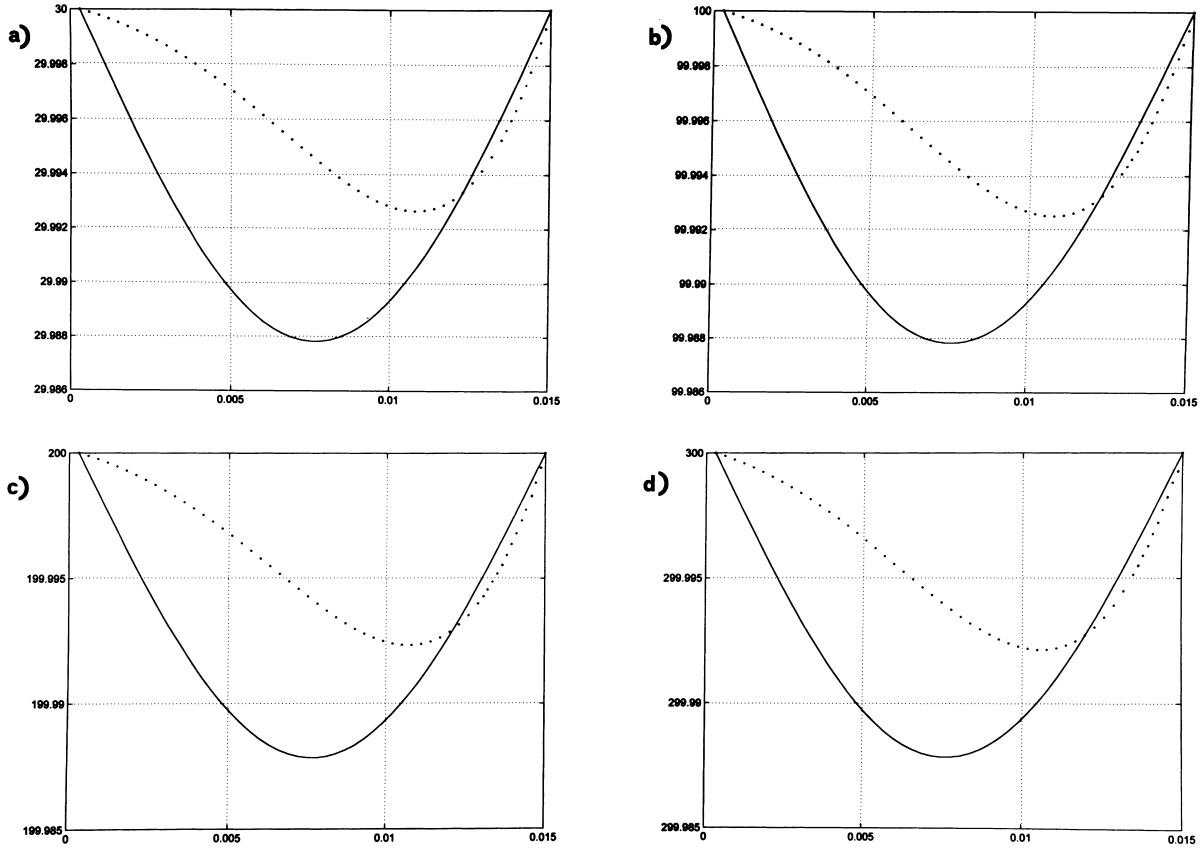

Fig. 10. Lactose concentration profiles into the membrane in absence of catalysis under isothermal (full lines) and non-isothermal (dotted lines) conditions. Initial lactose concentrations: (a) 30 mM; (b) 100 mM; (c) 200 mM; (d) 300 mM. On the y axis are reported the concentrations (mM) and on the x axis the membrane thickness.

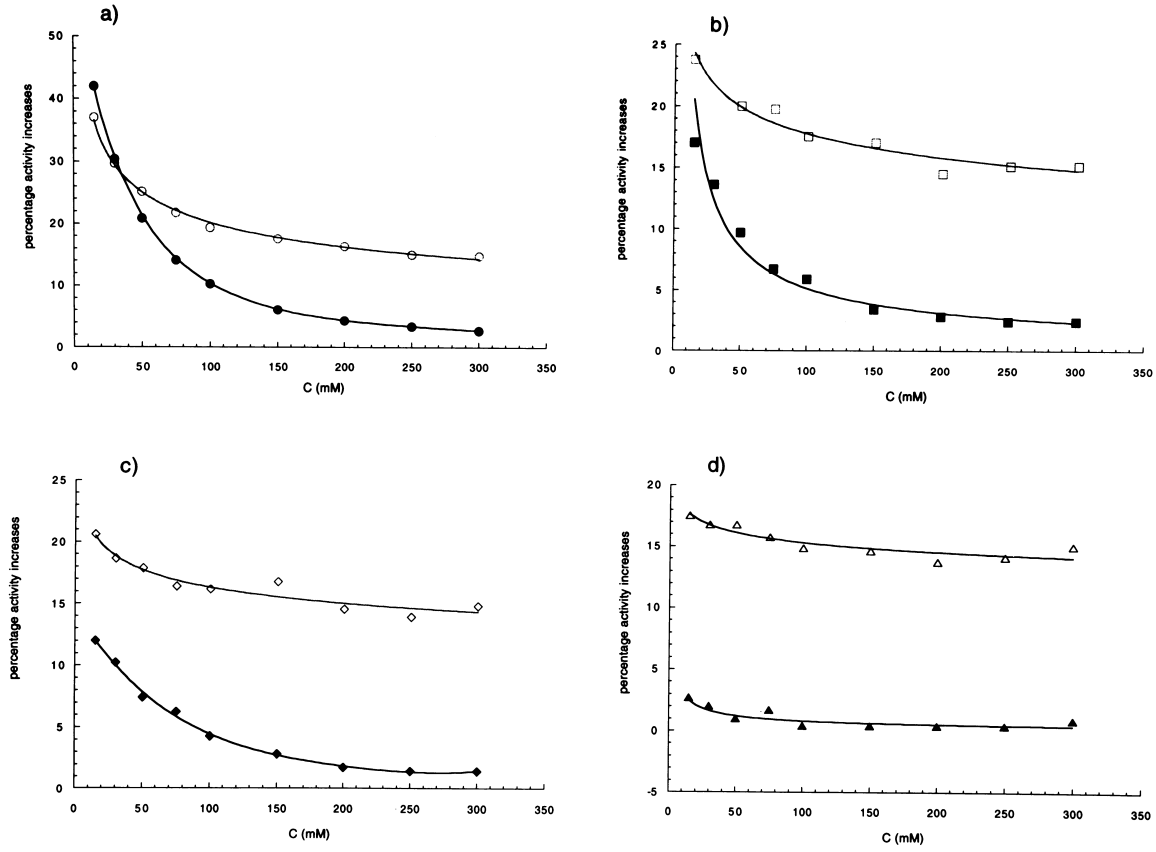

Fig. 11. Percentage increases of the enzyme reaction rates as a function of substrate concentration. Open symbols represent the experimental values; full symbols the simulation values. Each plot refers to a $\Delta T = 30$°C, while the average temperatures are: (a) $T_{av} = 25$°C; (b) $T_{av} = 30$°C; (c) $T_{av} = 35$°C; (d) $T_{av} = 40$°C .

non-isothermal condition. It is therefore a quantity analogous to the coefficient α', introduced in Eq. (12).

In Fig. 11a the values of β, full symbols, calculated according to expression (19), are reported as a function of substrate concentration, at $T_{av} = 25$°C. In the Figure the values of α', open symbols, are also reported to help the comparison. Results in the figure show the same trend for β and α', confirming that the process of thermodialysis plays a relevant role in increasing the activity of a catalytic membrane in a bioreactor operating under non-isothermal conditions. Fig. 11 b, c and d give the same information, but for the average temperatures of 30, 35 and 40°C. All the figures show β values smaller than the ones of α'. A possible cause for these differences is the circumstance that we have neglected the contribution to percentage activity increase due to dynamic and conformational changes in the protein structure induced by the flux of thermal energy (2,3).

4. Conclusion

The aim of the paper has been reached since the role of the process of thermodialysis in increasing the activity of a catalytic membrane has been demonstrated.

When lactose fluxes under non-isothermal conditions are compared with the catalytic activity exhibited by the same membrane, loaded with the enzyme, the same trends are observed under the same experimental conditions of concentration, average tempera-

ture and temperature difference. This circumstance results evident by comparing Figs. 3a and 7.

In the same way, when the values of substrate fluxes under isothermal and non-isothermal conditions are used in mass balance equations into the catalytic membrane, the solution of these equations by computer simulation gives concentration profiles into the membrane thickness which evidence the role of thermodialysis. What is observed is an increase of the substrate concentration profile inside the membrane (Fig. 10) under non-isothermal conditions in absence of catalysis, and vice versa a decrease (Fig. 9) of this profile when catalysis is present. This means that under non-isothermal conditions the enzymes immobilized into the membrane 'encounter' an effective higher substrate concentration than that occurring under isothermal conditions, and consequently they work also at a higher rate in presence of temperature gradients.

The result is that the percentage increases of the activity of the catalytic membrane experimentally found as a function of the initial substrate concentration show the same trend of those calculated by computer simulation using the measured substrate fluxes. This correspondence is indicative of a common physical cause responsible for the increase of the activity of a catalytic membrane in a bioreactor operating under non-isothermal conditions, this cause being the process of thermodialysis.

Acknowledgements

This work was partially supported by the Target Project 'Biotechnology' of CNR, by MURST (ex 40% founds), by MURST/CNR (5% founds: 'Programma Biotecnologie') and by the 'Regione Campania' in force of the law 41/94.

We are also grateful to the International Centre for Genetic Engineering and Biotechnology (ICGEB) which supported with a fellowship the activity of M. M. El-Masry at IIGB in Naples.

References

[1] D.G. Mita, M.A. Pecorella, P. Russo, S. Rossi, U. Bencivenga, P. Canciglia, F.S. Gaeta, J. Membr. Sci. 78 (1993) 69.
[2] D.G. Mita, M. Portaccio, P. Russo, S. Stellato, G. Toscano, U. Bencivenga, P. Canciglia, A. D'Acunto, N. Pagliuca, S. Rossi, F.S. Gaeta, Biotechnol. Appl. Biochem. 22 (1995) 281.
[3] M. Portaccio, S. Stellato, S. Rossi, U. Bencivenga, F. Palumbo, F.S. Gaeta, D.G. Mita, Biotechnol. Appl. Biochem. 24 (1996) 25.
[4] P. Russo, A. Garofalo, U. Bencivenga, S. Rossi, D. Castagnolo, A. D'Acunzo, F.S. Gaeta, D.G. Mita, Biotechnol. Appl. Biochem. 23 (1996) 141.
[5] P. Russo, A. De Maio, A. D'Acunzo, A. Garofalo, U. Bencivenga, S. Rossi, R. Annicchiarico, F.S. Gaeta, D.G. Mita, Research in Microbiology 148 (1997) 271.
[6] S. Stellato, M. Portaccio, S. Rossi, U. Bencivenga, G. La Sala, G. Mazza, F.S. Gaeta, D.G. Mita, J. Membr. Sci. 129 (1997) 175.
[7] F. Febbraio, M. Portaccio, S. Stellato, S. Rossi, U. Bencivenga, R. Nucci, M. Rossi, F.S. Gaeta, D.G. Mita, Biotechnol. Bioeng. 59 (1998) 108.
[8] M.S. Mohy Eldin, A. De Maio, S. Di Martino, M. Portaccio, S. Stellato, U. Bencivenga, S. Rossi, M. Santucci, P. Canciglia, F.S. Gaeta, D.G. Mita, J. Membr. Sci. 146 (1998) 237.
[9] M.S. Mohy Eldin, A. De Maio, S. Di Martino, N. Diano, V. Grano, N. Pagliuca, S. Rossi, U. Bencivenga, F.S. Gaeta, D.G. Mita, J. Membr. Sci. 47 (1999) 1.
[10] M.M. El-Masry, A. De Maio, S. Di Martino, U. Bencivenga, S. Rossi, B.A. Manzo, P. Pagliuca, P. Canciglia, M. Portaccio, F.S. Gaeta, D.G. Mita, J. Mol. Catal. B: Enzymatic. 9 (2000) 231.
[11] M.S. Mohy Eldin, M. Santucci, S. Rossi, U. Bencivenga, P. Canciglia, F.S. Gaeta, J. Tramper, A.E.M. Janssen, C.G.P.H. Schroen, D.G. Mita, J. Mol. Catal. B: Enzymatic 8 (2000) 221.
[12] M. Santucci, M. Portaccio, S. Rossi, U. Bencivenga, F.S. Gaeta, D.G. Mita, Biosens. Bioelectron. 14 (1999) 737.
[13] M. Santucci, M. Portaccio, M.S. Mohy Eldyn, N. Pagliuca, S. Rossi, U. Bencivenga, F.S. Gaeta, D.G. Mita, Enzyme Microb. Technol. 26 (2000) 593.
[14] F. Bellucci, M. Bobik, E. Drioli, F.S. Gaeta, D.G. Mita, G. Orlando, J. Chem. Eng. 56 (1978) 698.
[15] D.G. Mita, F. Bellucci, M.G. Cutuli, F.S. Gaeta, J. Phys. Chem. 86 (1982) 2975.
[16] N. Pagliuca, D.G. Mita, F.S. Gaeta, J. Membr. Sci. 14 (1983) 31.
[17] N. Pagliuca, U. Bencivenga, D.G. Mita, G. Perna, F.S. Gaeta, J. Membr. Sci. 33 (1987) 1.
[18] F.S. Gaeta, E. Ascolese, U. Bencivenga, J.M. Ortiz de Zarate, N. Pagliuca, G. Perna, S. Rossi, D.G. Mita, J. Phys. Chem. 96 (1992) 6342.
[19] F.S. Gaeta, Phys. Rev. 182 (1969) 289.
[20] F.S. Gaeta, F. Peluso, C. Albanese, D.G. Mita, Physical Rev. E 49 (1994) 433.
[21] I. Prigogine, Thermodynamics of Irreversible Processes, Interscience, New York, 1954.
[22] S.R. De Groot, P. Mazur, Non-equilibrium Thermodynamics, North-Holland, Amsterdam, 1962.
[23] R. Haase, Thermodynamics of Irreversible Processes, Addison-Wesley, Reading, MA, 1969.

[24] S.R. De Groot, Diffusion thermique dans les phases condesées, Amsterdam, 1945.
[25] F.S. Gaeta, G. Perna, G. Scala, F. Bellucci, J. Phys. Chem. 86 (1982) 2967.
[26] K.F. Alexander, W. Wirtz, Z. Phys. Chem. 195 (1950) 165.
[27] R. Haase, C. Steinert, Z. Phys. Chem. NF 21 (1959) 270.
[28] C.W. Carr, K. Sollner, J. Electrochem. Soc. 109 (1962) 616.
[29] R.P. Rastogi, R.L. Blokhra, R.K. Agarval, Trans. Faraday Soc. 60 (1964) 1386.
[30] R.P. Rastogi, K. Singh, Trans. Faraday Soc. 62 (1966) 1754.
[31] R. Haase, Z. Phys. Chem. 70 (1970) 1080.
[32] M.S. Dariell, O. Kedem, J. Phys. Chem. 79 (1971) 1773.
[33] W.E. Goldstein, F.H. Verhoff, AIChE J. 21 (1975) 229.
[34] H. Vink, S.A.A. Chishti, J. Membr. Sci. 1 (1976) 149.
[35] J.I. Mengual, F.G. Lopez, C. Fernandez-Pineda, J. Membr. Sci. 26 (1986) 211.
[36] E. Drioli, Y. Wu, Desalination 53 (1985) 339.
[37] G.C. Sarti, C. Costoli, Membranes and Membranes Processes, in: E. Drioli and M. Nakagaki (Eds.), Plenum Press, New York, 1986, 349.
[38] R.W. Schofield, A.G. Fane, C.J.D. Fell, J. Membr. Sci. 33 (1987) 299.
[39] R.W. Schofield, A.G. Fane, C.J.D. Fell, J. Membr. Sci. 53 (1990) 173.
[40] M.M. El-Masry, A. De Maio, S. Di Martino, V. Grano, S. Rossi, N. Pagliuca, Z.H. Abd El-Latif, A.B. Moustafa, A. D'Uva, S. Gaeta, D.G. Mita, Influence of the non-isothermal conditions on the activity of enzymes immobilized on nylon grafted membranes, J. Mol. Catal. B Enzyme 11 (2000) 113.